

Binding Mode of CA074, a Specific Irreversible Inhibitor, to Bovine Cathepsin B as Determined by X-Ray Crystal Analysis of the Complex

Atsushi Yamamoto,^{*1} Tadaoki Hara,^{*} Koji Tomoo,^{*} Toshimasa Ishida,^{*2} Tomomi Fujii,[†] Yasuo Hata,[‡] Mitsuo Murata,[‡] and Kunihiro Kitamura[‡]

^{*}Osaka University of Pharmaceutical Sciences, 4-20-1 Nasahara, Takatsuki, Osaka 569-11; [†]Institute for Chemical Research, Kyoto University, Gokasho, Uji, Kyoto 611; and [‡]Research Center, Taisho Pharmaceutical Co., Ltd., 1-403 Yoshino-cho, Ohmiya, Saitama 330

Received for publication, January 9, 1997

The binding mode of CA074 [*N*-(*L*-3-*trans*-propylcarbamoyl-oxirane-2-carbonyl)-*L*-isoleucyl-*L*-proline], a specific irreversible inhibitor, to bovine spleen cathepsin B was elucidated by X-ray crystal structure analysis of the complex at 2.2 Å resolution (conventional $R=0.185$). Inconsistently with our model used for the development of CA074, the *L*-isoleucyl-*L*-proline and propylcarbamoyl moieties are located at the *S'* and *S* subsites, respectively. This unexpected binding is primarily due to (i) similar extended chain conformations (due to the same *S* configurations) at the oxirane C2 and C3 atoms of CA074 and (ii) the just fit formation of double hydrogen bonds between the carboxyl oxygens of *L*-proline and the imidazole nitrogens of His-110 and His-111 residues (these residues are missing in papain, the tertiary structure of which was used for the design of CA074). The oxirane C3 atom possessing the *P'* substituent is covalently bound to the Cys-29 S γ atom (C3-S γ =1.79 Å) and the *S* configuration is maintained. The present result will provide useful information for characterizing the substrate-specificity of cathepsin B.

Key words: CA074, cathepsin B, complex, crystal structure, irreversible inhibitor.

Lysosomal cysteine proteases are abundant in living cells and play important roles in intracellular proteolysis (1). Cathepsin B [EC 3.4.22.1] is a major component of lysosomal enzymes and has been implicated in muscular dystrophy (2), bone resorption (3), pulmonary emphysema (4), rheumatoid arthritis (5), and tumor metastasis (6). Since the overexpression of cathepsin B could cause such serious diseases, cathepsin-specific inhibitors should serve as therapeutic drugs for these diseases.

Recently we developed a selective inhibitor of cathepsin B, CA074 [*N*-(*L*-3-*trans*-propylcarbamoyloxirane-2-carbonyl)-*L*-isoleucyl-*L*-proline] (7), which was designed based on the tertiary structure of a cathepsin B-epoxysuccinyl peptide complex predicted from the crystal structure of papain-E-64-c (a typical inhibitor for a wide variety of thiol proteases) complex (8); CA074 was experimentally proven to be a specific inhibitor of cathepsin B *in vivo* (9) as well as *in vitro* (10), and is now widely used as a probe to clarify the biological function of cathepsin B (11-13). In order to examine the actual binding mode of CA074 to cathepsin B, we analyzed the structure of bovine cathepsin B-CA074 complex by X-ray crystallography; the crystallization and the preliminary crystallographic data have already been reported (14). This paper focuses on why CA074 exhibits selective inhibition for cathepsin B, based on comparison with the binding mode of E-64-c-papain

complex. The chemical structures of E-64-c and CA074 are given in Fig. 1. Recently, the crystal structures of human cathepsin B-CA030 (a related inhibitor) complex (15) and recombinant rat cathepsin B-benzyloxy-carbonyl-Arg-Ser(OBzl)-chloromethylketone complex (16) have been reported. These results, together with the proposed binding models of E-64 derivatives to cathepsin B (17, 18), are also useful for characterizing the substrate-specificity of cathepsin B.

MATERIALS AND METHODS

Crystallization and Data Collection—The preparation of bovine spleen cathepsin B-CA074 complex and the crystallization of this complex by vapor diffusion at 20°C have been reported previously (14). Bipyramidal complex crystals with maximum dimensions of 0.7×0.3×0.3 mm appeared within three weeks. The X-ray diffraction data up to 2.2 Å resolution were collected on an imaging plate detector (R-AXIS IIc) with a Rigaku rotating-anode X-ray source using Ni-filtered Cu K α radiation at room temperature.

Potential heavy-atom derivatives of the complex crystals were prepared by direct addition of one of several dozen heavy-atom solutions to small drops with freshly grown crystals. Of the numerous heavy-atom derivative replacement experiments, only two produced interpretable diffraction changes.

Structure Determination and Refinement—Space group, unit-cell constants and data collection are summarized in Table I. The heavy-metal sites of derivatives were located by manual inspection of the difference Patterson maps and

¹ Present address: Pharmaceutical Technology Division, Tanabe Seiyaku Co., Ltd., 3-16-89 Kashima, Yodogawa-ku, Osaka 532.

² To whom correspondence should be addressed. Tel: +81-726-90-1068, Fax: 81-726-90-1005, E-mail: ishida@oysun01.oups.ac.jp

by cross-phased difference Fourier maps, and were then refined using PHASES (19) (Table II). After this procedure the figure of merit for the MIR (multiple isomorphous replacement) phases was 0.547 (3.0 Å). The final refined heavy atom parameters are summarized in Table III. These MIR phases were improved by solvent flattening procedure. All structures were refined by iterative cycles of manual rebuilding using the program FRODO (20) and simulated annealing refinement using the program X-

TABLE I. Summary of crystal data, and data collection statistics.

Space group	$P4_32_12$
Cell constants	$a = b = 70.48 \text{ \AA}$, $c = 143.9 \text{ \AA}$
Resolution	2.18 Å
No. of observations	98,228
No. of independent reflections	32,123
Completeness	82.1%
R_{merge}	6.69%
No. of complexes in asymmetric unit	1

$R_{\text{merge}} = \frac{\sum \sum |I(hkl) - \langle I(hkl) \rangle|}{\sum \sum I(hkl)}$ and the overall agreement between reflections measured more than once.

TABLE II. Summary of phasing analysis.

Derivative	Hg(AcO) ₂	K ₂ PtCl ₆
Soaking concentration	1 mM	2 mM
Soaking time	4 days	16 h
Resolution	3 Å	3 Å
No. of observations	15,474	14,326
No. of independent reflections	7,488	6,122
Completeness	74.4%	72.5%
R_{merge}	8.29%	7.89%
Phasing power ^a	2.09	1.71
R_{KRAUT}^b	0.061	0.114
No. of sites	4	4
R_{iso}^c	0.069	0.107

^aPhasing power = $F_H(\text{calc})/E$ for the isomorphous difference. E is the estimated error. ^b $R_{\text{KRAUT}} = \frac{\sum |F_{PH}(\text{obs}) - |F_{PH}(\text{calc})||}{\sum |F_{PH}(\text{obs})|}$ with the sum taken over all acentric reflections. ^c $R_{\text{iso}} = \frac{\sum ||F_{PH}| - |F_P||}{\sum |F_P|}$.

PLOR (21). During refinement the resolution was gradually increased up to 2.2 Å. The R -value of the present model is 0.185 for 17,671 independent reflections from 7.0 to 2.2 Å resolution, where 251 out of 253 amino acid residues and 88

TABLE III. Heavy atom parameters.

Derivative	x	y	z	Occupancy	Ligands
Hg(AcO) ₂	0.347	0.123	-0.056	0.704	Cys-240, His-239
	0.282	0.134	0.045	0.186	His-199
	0.300	0.114	0.933	0.189	Cys-240
K ₂ PtCl ₆	0.249	0.065	0.038	0.133	His-111
	0.106	0.042	0.833	0.833	Met-161, Lys-158
	0.232	0.085	0.710	0.565	Met-150
	0.213	0.036	0.018	0.321	Met-196
	0.602	0.089	0.463	0.110	His-97, Ser-96

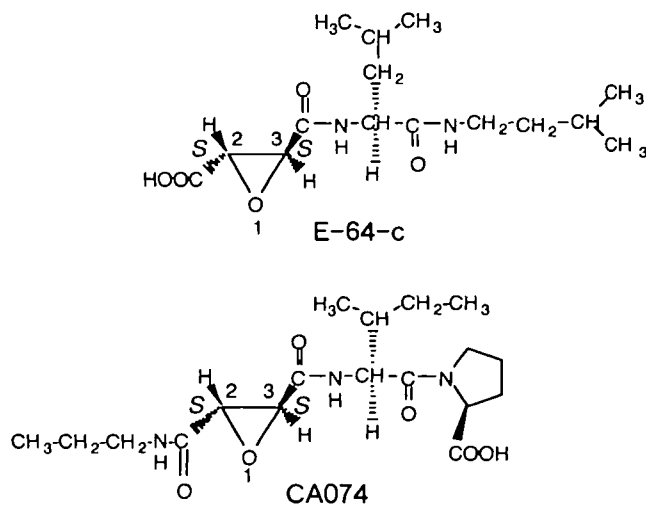


Fig. 1. Chemical structures of E-64-c and CA074, together with the atomic numbering and configuration of the oxirane ring. CA074 was developed from E-64-c complexed with papain.

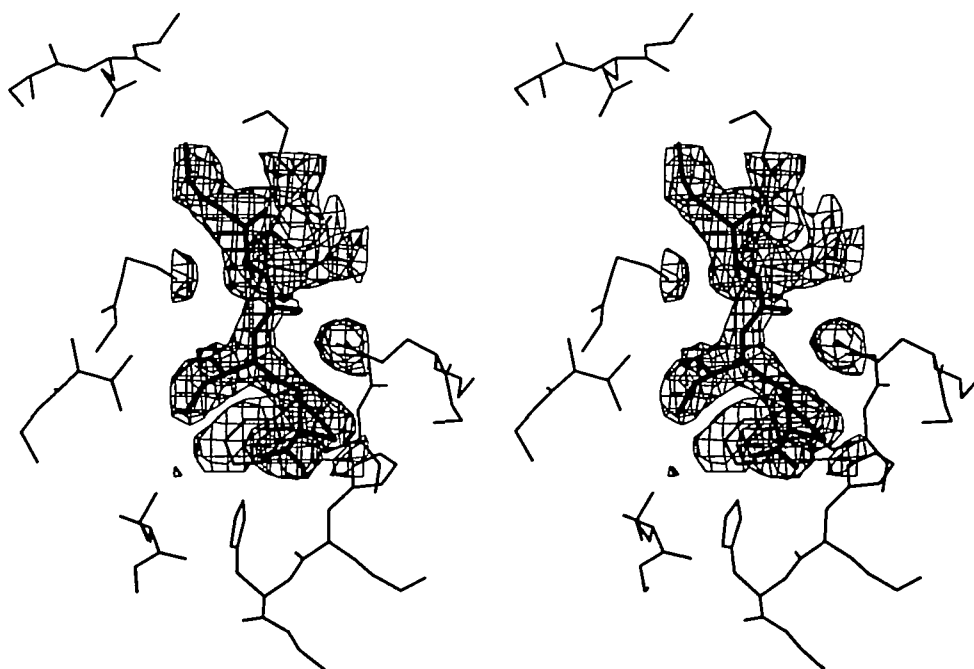


Fig. 2. Stereoscopic $2F_o - F_c$ electron density map (1σ level) of CA074 binding to the cathepsin B in the final stage of refinement. The position of CA074 on the map is shown with thick lines. Thin lines represent the partial structure of the cathepsin B around the active site.

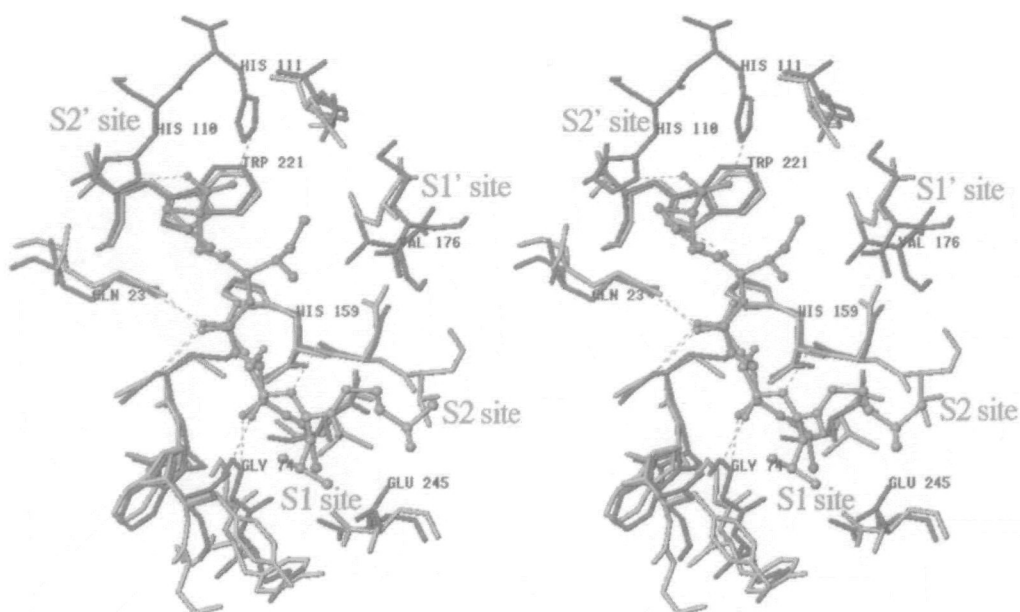
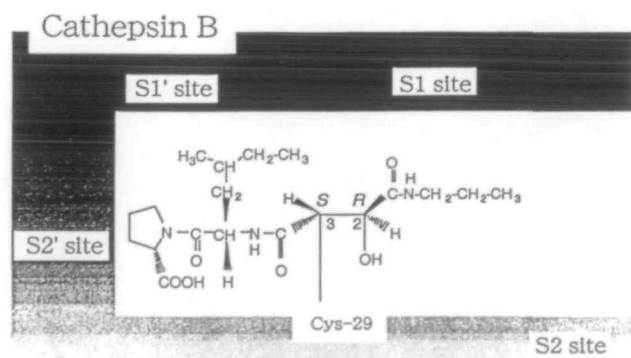


Fig. 3. Stereoscopic comparison between the binding modes of CA074 (red) and E-64-c (blue) inhibitors which are covalently bonded to cathepsin B (green) and papain (brown), respectively. By reference to the literature (22), the topologically equivalent amino acid residues of both enzymes are shown. Broken lines represent hydrogen bonds.

(a) CA074



(b) E-64-c

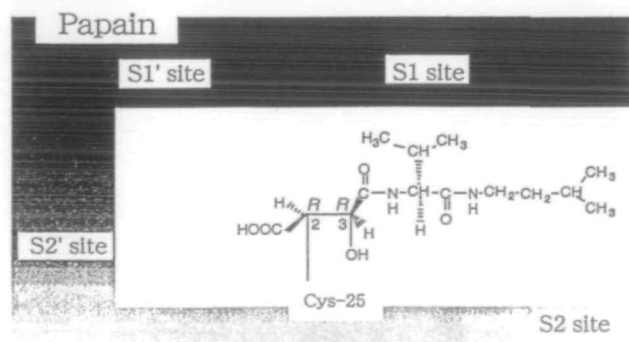


Fig. 4. Schematic of the configuration around the CA074 (a) or E-64-c (b) oxirane C2 and C3 atoms caused by the covalent bond formation with the S γ atom of the cathepsin B Cys-29 or papain Cys-25 residue, respectively. The actual binding topologies (S or S' subsites) of their inhibitors to the respective enzymes are also shown.

water molecules are included. The atomic coordinates have been deposited in the Brookhaven Protein Data Bank.

RESULTS AND DISCUSSION

The present crystal contains one complex per asymmetric unit, which is a notable feature because the crystals of native or inhibited cathepsin B analyzed to date (15, 16, 22) contain two molecules per asymmetric unit. Bovine spleen cathepsin B consists of a light chain of Lys-1-Arg-49 and a heavy chain of Val-50-Thr-253 (23), and has seven disulfide bridges (24). However, no electron density was observed for the Gly-48-Arg-49 residues, while the other residues were traced by the relatively well-defined density. The overall structure of the present cathepsin B closely resembles that of human liver cathepsin B (PDB code: 1HUC) (22), although the former enzyme has one additional disulfide bond.

The electron density map of CA074 at the active site of cathepsin B is shown in Fig. 2, where a possible binding conformation of the inhibitor is shown with thick lines. The L-isoleucyl-L-proline and propylcarbamoyl moieties of CA074 are situated at the S' and S subsites of the enzyme, respectively. This binding mode is opposite to what we supposed: we supposed the reverse binding mode for the molecular design of CA074 based on the tertiary structure prediction of cathepsin B, which was constructed from the crystal structure of the papain-E-64-c complex (8). A comparison between the binding modes of inhibitors in the cathepsin B-CA074 and papain-E-64-c complexes is shown in Fig. 3. It is obvious that the L-proline, L-isoleucyl, carbamoyl, and propyl moieties of CA074 correspond to the P2', P1', P1, and P2 substituents, respectively, in the similar manner as the proposed models (15, 17, 18). As the main reasons why the L-isoleucyl-L-proline moiety of CA074 preferred to bind at the S' subsites, though the cathepsin B has sufficient space to accommodate this moiety at S subsites, the followings can be proposed: (i) the same S configurations of the oxirane C2 and C3 atoms allow the collinear arrangement of the L-isoleucyl-L-proline and

propylcarbamoyl moieties, which is suitable for tight binding of the inhibitor to the cathepsin B binding cleft, and (ii) the just fit formation of double hydrogen bonds between the carboxyl oxygens of the C-terminal Pro and the imidazole nitrogens of His-110 and His-111 residues (these are missing in papain)—similar binding has been observed for CA030, a related inhibitor (15). On the other hand, the propylcarbamoyl moiety of CA074 is located at the S1 and S2 sites. The carbonyl O is hydrogen-bonded to Gly-74 NH, and the amide NH could participate in hydrogen bonding with Gly-198 O by slight structural change, because the distance is close to the range of hydrogen bond [$\approx 4.02 \text{ \AA}$].

The electron density shows the covalent bond formation between the oxirane C3 atom of CA074 and the Cys-29 S γ atom (C3-S γ = 1.79 \AA) (Fig. 2). The S configuration at the oxirane C3 atom is maintained during the σ -covalent bond formation (Fig. 4), although it is not definitive because of the nearly planar density around the C3 atom; the chirality change of S to R at the C2 atom is due to the change of ranking order of the substituents. Concerning the covalent bond formation, on the other hand, the nucleophilic attack of the Cys S γ atom on the oxirane carbon atom appears to occur according to a universal rule that the Cys S γ atom attacks the oxirane carbon atom possessing the P' substituents (C3 for CA074-cathepsin B and C2 for E-64-c-papain).

REFERENCES

- Kirschke, H. and Barrett, A.J. (1987) Chemistry of lysosomal proteases in *Lysosomes: Their Role in Protein Breakdown* (Glauermann, H. and Ballard, F.J., eds.) pp. 193-283, Academic Press, London, UK
- Katunuma, N. and Kominami, E. (1987) Distributions and localizations of lysosomal cysteine proteinases and cystatins. *Rev. Physiol. Biochem. Pharmacol.* **108**, 1-20
- Dalaisse, J.M., Eeckhout, Y., and Vaes, G. (1984) *In vivo* and *in vitro* evidence for the involvement of cysteine proteinases in bone resorption. *Biochem. Biophys. Res. Commun.* **125**, 441-447
- Johnson, D. and Travis, J. (1977) Inactivation of human α_1 proteinase inhibitor by thiol proteinases. *Biochem. J.* **163**, 639-641
- Werb, Z. (1989) Proteinases and matrix degradation in *Textbook of Rheumatology* (Keller, W.N., Harris, E.D., Ruddy, S., and Sledge, C.S., eds.) pp. 300-321, W.B. Saunders Co., Philadelphia, PA
- Sloane, B.F., Rozhin, J., Robinson, D., and Honn, K.V. (1990) Role for cathepsin B and cystatins in tumor growth and progression. *Biol. Chem. Hoppe-Seyler* **371** (Suppl.), 193-198
- Sumiya, S., Yoneda, T., Kitamura, K., Murata, M., Yokoo, C., Tamai, M., Yamamoto, A., Inoue, M., and Ishida, T. (1992) Molecular design of potent inhibitor specific for cathepsin B based on the tertiary structure prediction. *Chem. Pharm. Bull.* **40**, 299-303
- Yamamoto, D., Matsumoto, K., Ohishi, H., Ishida, T., Inoue, M., Kitamura, K., and Mizuno, H. (1991) Refined X-ray structure of papain-E-64-c complex at 2.1 \AA resolution. *J. Biol. Chem.* **266**, 14771-14777
- Towatari, T., Nikawa, T., Murata, M., Yokoo, C., Tamai, M., Hanada, K., and Katunuma, N. (1991) Novel epoxysuccinyl peptides: A selective inhibitor of cathepsin B, *in vivo*. *FEBS Lett.* **280**, 311-315
- Murata, M., Miyashita, S., Yokoo, C., Tamai, M., Hanada, K., Hatayama, K., Towatari, T., Nikawa, T., and Katunuma, N. (1991) Novel epoxysuccinyl peptides: Selective inhibitors of cathepsin B, *in vitro*. *FEBS Lett.* **280**, 307-310
- Buttle, D.J., Murata, M., Knight, C.G., and Barrett, A.J. (1992) CA074 methyl ester: A proinhibition for intracellular cathepsin B. *Arch. Biochem. Biophys.* **290**, 377-380
- Ohshita, T., Nikawa, T., Towatari, T., and Katunuma, N. (1992) Effects of selective inhibition of cathepsin B and general inhibition of cysteine proteinases on lysosomal proteolysis in rat liver *in vitro* and *in vivo*. *Eur. J. Biochem.* **209**, 223-231
- Werle, B., Ebert, W., Klein, W., and Spiess, E. (1995) Assessment of cathepsin L activity by use of the inhibitor CA-074 compared to cathepsin B activity in human lung tumor tissue. *Biol. Chem. Hoppe-Seyler* **376**, 157-164
- Yamamoto, A., Kaji, T., Tomoo, K., Ishida, T., Inoue, M., Murata, M., and Kitamura, K. (1992) Crystallization and preliminary X-ray study of the cathepsin B complexed with CA074, a selective inhibitor. *J. Mol. Biol.* **227**, 942-944
- Turk, D., Podobnik, M., Popovic, T., Katunuma, N., Bode, W., Huber, R., and Turk, V. (1995) Crystal structure of cathepsin B inhibited with CA030 at 2.0 \AA resolution: A basis for the design of specific epoxysuccinyl inhibitors. *Biochemistry* **34**, 4791-4797
- Jia, Z., Hasnain, S., Hirama, T., Lee, X., Mort, J.S., To, R., and Huber, C.P. (1995) Crystal structures of recombinant rat cathepsin B and a cathepsin B-inhibitor complex. *J. Biol. Chem.* **270**, 5527-5533
- Gour-Salin, B.J., Lachance, P., Plouffe, C., Storer, A.C., and Menard, R. (1993) Epoxysuccinyl dipeptides as selective inhibitors of cathepsin B. *J. Med. Chem.* **36**, 720-725
- Klinkert, M., Cioli, D., Shaw, E., Turk, V., Bode, W., and Butler, R. (1994) Sequence and structure similarities of cathepsin B from the parasite *Schistosoma mansoni* and human liver. *FEBS Lett.* **351**, 397-400
- Furey, W. and Swaminathan, S. (1990) PHASES A program package for the processing and analysis of diffraction data from macromolecules. *Am. Crystallogr. Assoc. Meeting Abstr. Ser. 2*, 18-73
- Jones, T.A. (1978) A graphics model building and refinement system for macromolecules. *J. Appl. Crystallogr.* **11**, 268-272
- Brunger, A.T. (1992) X-Plor Manual Version 3.1, Yale University, New Haven, CT
- Musil, D., Zucic, D., Turk, D., Engh, R.A., Mayr, I., Huber, R., Popovic, T., Turk, V., Towatari, T., Katunuma, N., and Bode, W. (1991) The refined 2.15 \AA X-ray crystal structure of human liver cathepsin B: the structural basis for its specificity. *EMBO J.* **10**, 2321-2330
- Meloun, B., Baudys, M., Pohl, J., Pavlik, M., and Kostka, V. (1988) Amino acid sequence of bovine spleen cathepsin B. *J. Biol. Chem.* **263**, 9087-9093
- Baudys, M., Meloun, B., Gan-Erdene, T., Pohl, J., and Kostka, V. (1990) Disulfide bridges of bovine spleen cathepsin B. *Biol. Chem. Hoppe-Seyler* **371**, 485-491